On the role of buoyancy force in the ore genesis of SEDEX deposits: Example from Northern Australia

YANG JianWen[1,2†], FENG ZuoHai[1], LUO XianRong[1] & CHEN YuanRong[1]

[1] Department of Resources and Environmental Engineering, Guilin University of Technology, Guilin 541004, China;
[2] Department of Earth and Environmental Sciences, University of Windsor, Ontario N9B 3P4, Canada

Finite element modeling on a highly conceptualized 2-D model of fluid flow and heat transport is undertaken to simulate the paleo-hydrological system as if the Mount Isa deposits were being formed in the Mount Isa basin, Northern Australia, and to evaluate the potential of buoyancy force in driving basin-scale fluid flow for the formation of sedimentary-exhalative (SEDEX) deposits. Our numerical case studies indicate that buoyancy-driven fluid flow is controlled mainly by the fault penetration depth and its spatial relation with the aquifer. Marine water recharges the basin via one fault and flows through the aquifer where it is heated from below. The heated metalliferous fluid discharges to the basin floor via the other fault. The venting fluid temperatures are computed to be in the range of 115 to 160℃, with fluid velocities of 2.6 to 4.1 m/year over a period of 1 Ma. These conditions are suitable for the formation of a Mount Isa-sized zinc deposit, provided a suitable chemical trap environment is present. Buoyancy force is therefore a viable driving mechanism for basin-scale ore-forming hydrothermal fluid migration, and it is strong enough to lead to the genesis of supergiant SEDEX deposits like the Mount Isa deposit, Northern Australia.

hydrothermal fluid flow, finite element modeling, SEDEX deposits, Mount Isa basin

Sedimentary-exhalative (SEDEX) deposits are a major source of lead and zinc, and an important source of silver. On the global scale, they account for about 40% of zinc production and about 60% of lead production[1]. Geological and sulphide paragenetic studies suggest that this type of deposits may be formed by hydrothermal exhalative processes of metal-bearing brines discharging onto the basin floor. Despite this general understanding, geologists continue to debate the mechanisms of fluid migration, heat flow and mass transport for ore deposition.

Several factors have been deemed responsible for basin-scale fluid flow, including topography, compaction, buoyancy, and deformation[2]. Among these, buoyancy driven flow is potentially of great importance because it can lead to fluid flow and mass transport over large distances and significantly shorter time scales, compared with diffusion alone. This is because diffusion results from molecular collision, representing a micro-scale process. In certain circumstances, buoyancy may become even more important than other forces in enhancing hydrodynamic mixing of the dense fluid with the less dense ambient groundwater[3].

A buoyancy force results from variations in fluid density due to spatial and temporal changes in temperature and salinity. Buoyancy driven fluid circulation is commonly termed free convection because of the lack of external inputs and outputs[4]. The importance of this type of fluid flow has long been recognized in mid-ocean ridge hydrothermal systems[5,6], seawater intrusion[7,8], and solute transport[9,10]. Recently, buoyancy-

driven free convection models become more popular as one of the most likely hydrological scenarios for SEDEX formation[11]. For instance, Garven et al.[12] investigated the likely role of free convective fluid migration in the formation of the HYC deposit. Their numerical results exhibit a dominant recharge-discharge pattern controlled by syn-sedimentary faults and a subsurface sandstone aquifer. Yang et al.[13] simulated time-dependent fluid flow and developed criteria for efficient identification of potentially mineralizing discharge faults in sedimentary basins, and more recently Yang et al.[14] investigated the effect of salinity on ore-forming processes and fluid flow patterns.

The major aim of this paper is to evaluate whether buoyancy driven fluid flow and heat transport was a viable mechanism for the generation of SEDEX deposits. This will be done in the subsequent sections by numerical simulations corresponding to a highly conceptualized paleo-hydrological system pertinent to the genesis of shale-hosted lead-zinc ores in the Mount Isa basin, Northern Australia.

1 Governing equations and finite element modeling

Mathematically, hydrothermal fluid flow in sedimentary basins is governed by the fluid continuity equation and thermal energy conservation equation, coupled through Darcy's law. Equations of state are also required to define the temperature- and pressure-dependence of fluid density and viscosity. The fluid continuity equation can be expressed in term of a freshwater hydraulic head[7] for the variable density fluid flow system. A detailed description of these equations can be found in the literature[6,15]. If the porous medium is non-deformable and there exists a thermal equilibrium between the fluid and the solid matrix, the fluid continuity and thermal energy conservation equations can be expresses as

$$\frac{\partial}{\partial x}\left(K\frac{\partial h}{\partial x}\right)+\frac{\partial}{\partial y}\left(K\frac{\partial h}{\partial y}\right)+\frac{\partial}{\partial z}\left(K\frac{\partial h}{\partial z}+K\rho_r\right)=S_s\frac{\partial h}{\partial t},$$
(1)

and

$$\frac{\partial}{\partial x}\left(\lambda_m\frac{\partial T}{\partial x}\right)+\frac{\partial}{\partial y}\left(\lambda_m\frac{\partial T}{\partial y}\right)+\frac{\partial}{\partial z}\left(\lambda_m\frac{\partial T}{\partial z}\right)$$
$$-\frac{\partial}{\partial x}\left(c_w\rho_w q_x T\right)-\frac{\partial}{\partial y}\left(c_w\rho_w q_y T\right)-\frac{\partial}{\partial z}\left(c_w\rho_w q_z T\right)$$

$$=\left[c_w\rho_w\phi+c_s\rho_s(1-\phi)\right]\frac{\partial T}{\partial t},$$
(2)

where q_x, q_y and q_z are the Darcy flux components in the x, y and z directions, K the hydraulic conductivity, ϕ the porosity, $\lambda_m=\lambda_w^\phi\lambda_s^{1-\phi}$ (λ_w and λ_s denote the thermal conductivity of the fluid and solid phase), c_w and c_s the specific heat capacity of the fluid and solid phase, ρ_w and ρ_s the density of the fluid and solid phase, ρ_r the relative fluid density defined as $\rho_r=\rho_w/\rho_0-1$ (ρ_0 is the reference freshwater density), S_s the specific storage (dependent on the fluid density and compressibility, rock matrix compressibility, and porosity), t the time, h the freshwater head and T is the temperature. These equations form a time-dependent, nonlinear and coupled system, which leads to their solutions to become nontrivial even for a very simple 1-D geological system.

In the numerical solution of these equations, we employ a standard Galerkin finite element method[16,17]. Nonlinearities in the coupled equations are accommodated by centering the nonlinear terms in time and iterating the solution to a specified convergence tolerance. In brief, starting with the initial temperature and fluid flow conditions, we first update the fluid density and viscosity using the latest temperature data from the previous time step; then determine the equivalent freshwater head distribution by solving the fluid continuity equation; next calculate fluid velocity based on the Darcy equation using the updated fluid properties and equivalent freshwater head; and finally determine the temperature distribution by solving the thermal energy conservation equation. These iteration steps are repeated and not allowed to move on to the next time levels until the preset convergence criteria are satisfied. We adopt a non-orthogonal quadrilateral mesh to create finite elements since it is better suited for the complex geometry of different stratigraphic units and faults encountered in sedimentary basins. Each element is assigned permeability, porosity, thermal conductivity and other physical parameters governing fluid flow and heat transport based on the rock properties. The details of the computational method, both the principles and the schemes for their implementation into finite element software, can be found in our previous publications[6,18].

2 Conceptual hydrological model

Figure 1 illustrates the 2-D paleo-hydrological model,

which is constrained by some of the common features of a sedimentary basin's rift-and-sag phase, and in particular by the reconstructions of the Mount Isa basin, Northern Australia[19,20]. It represents the highly conceptualized and simplified subsurface stratigraphy and structure, which controlled the hydrological system when the Mount Isa SEDEX deposits were formed early in the history of the Mount Isa basin. As shown in Figure 1(a), the conceptual model involves a volcanic basement sequence of low permeability (Unit 4), a sandstone aquifer of high permeability (Unit 3), a rift cover sequence of intermediate permeability (Unit 2), and an upper cover sequence of shales and siltstones (Unit 1) that hosts mineral deposits formed during or soon after sediment deposition. Two more permeable faults (Fault 1 and Fault 2) are also included to penetrate from the upper

sequence into the basement. The faults are 1 km wide and steeply west-dipping, which is constrained by surface exposure and seismic profiling[21]. Grid discretization of the faults can be found in Figure 1(b). Similar general geological structure of the Mount Isa-McArthur basin region has been also used in previous fluid flow models[12−14,18,22,23]. Like in the previous studies[22,23], Fault 1 on the left is equivalent to the Mount Isa fault system, and Fault 2 on the right simulates a fault zone to farther north, such as the Termite Range fault at the Century deposit. The conceptual model has a dimension of 60 km×20 km and is discretised by a 2-D non-orthogonal quadrilateral mesh consisting of 52 element columns and 19 rows (Figure 1(b)).

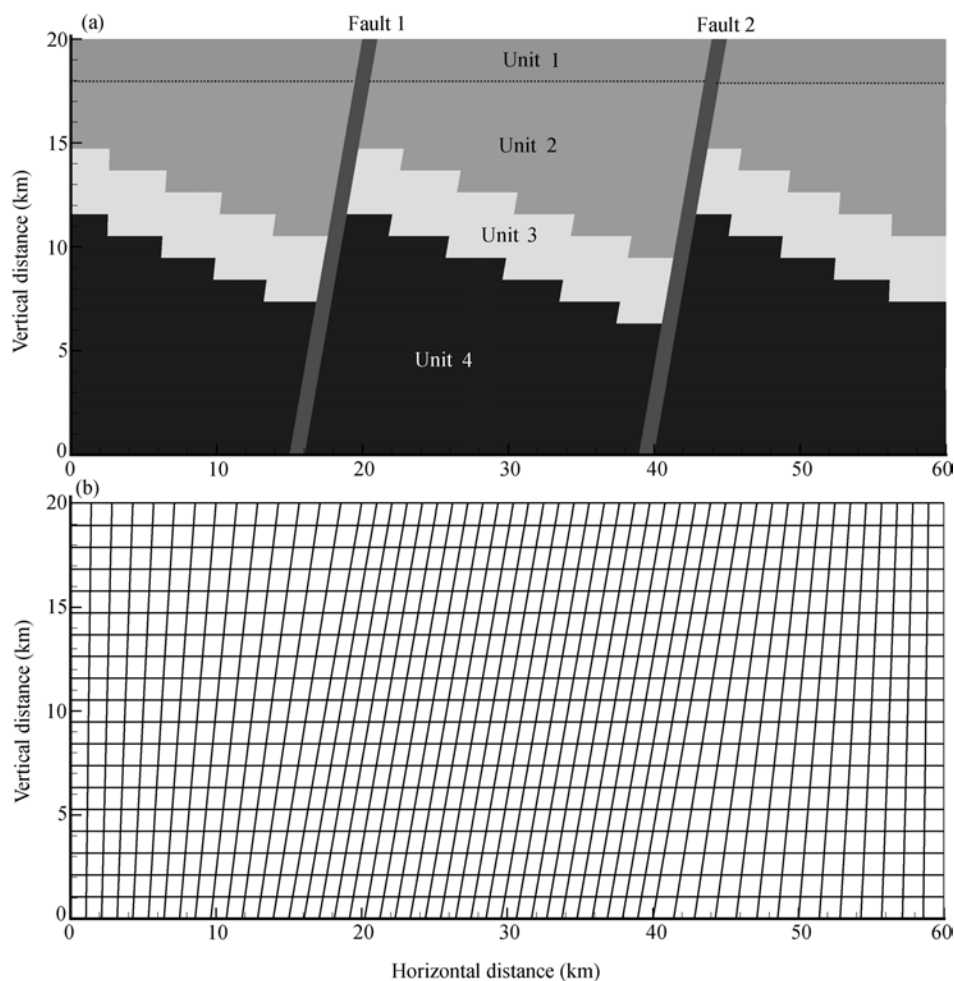The two steeply-dipping faults cut the sandstone aquifer (Unit 3), which forms a favorable hydrological

Figure 1 (a) Highly simplified model of titled and submerged rift blocks associated with the formation of SEDEX deposits of the Mount Isa basin, Northern Australia; (b) finite element mesh used in the 2-D fluid flow and heat transport modeling. See Table 1 for the hydrological and thermal properties assigned to the faults and rock units.

framework for regional-scale fluid flow. The permeabilities and thermal conductivities assigned to the stratigraphic elements and faults are given in Table 1, following the previous numerical investigations in the Mount Isa-McArthur basin region[13,14,18,22,23]. We assume that the vertical permeability of the host rocks is two orders of magnitude less than the horizontal one due to bedded and stratified nature of these sedimentary rocks. In addition, we assume c_w=4174 J·kg^{-1}·℃$^{-1}$, c_s=800 J·kg^{-1}·℃$^{-1}$, λ_w=0.5 W·m^{-1}·℃$^{-1}$, ρ_s=2630 kg/m^3, ρ_0=1000 kg/m^3, and ϕ=10%.

Table 1 Major physical parameters of the faults and host rocks

Hydrological unit and formation	Horizontal permeability (m^2)	Vertical permeability (m^2)	Thermal conductivity (J·m^{-1}·s^{-1}·℃$^{-1}$)
Fault	4×10^{-14}	4×10^{-14}	2.0
Unit 1	1×10^{-15}	1×10^{-17}	2.0
Unit 2	2×10^{-15}	2×10^{-17}	2.5
Unit 3	4×10^{-14}	4×10^{-16}	3.0
Unit 4	2×10^{-16}	2×10^{-18}	3.0

The upper boundary beside the faults, maintained at 20℃ following the previous numerical studies[12−14,18], is at the seafloor and permeable to fluid flow. Over the top of the faults, the vertical temperature gradient is fixed at zero. That is, the fluid is assumed to be isothermal near the top surface owing to fluid flow via the faults. The lower boundary is maintained at 450℃, justified by present-day heat flow measurements in Northern Australia (S. McLaren and M. Sandiford, personal communication). The bottom of the model is assumed impermeable since it lies within the deep volcanic basement. The side boundaries are assumed to be adiabatic to heat transfer and impermeable to fluid flow. The initial fluid velocity is set to zero over the whole solution domain, and the initial temperature is assumed to vary linearly with depth. In the following numerical case studies, the faults' penetration depth and boundary conditions will be adjusted.

3 Numerical modeling results

The first case study corresponds to the reference conditions specified above and given in Figure 1 and Table 1. Figure 2 shows the temperature and fluid velocity distribution at different time levels. The modeling reveals that the cold seawater penetrates downwards along Fault 2 and then flows laterally, mainly through the permeable aquifer but with a little via the less permeable basement

sequence at depth. In the meantime, the fluid is heated up from below. Basinal fluid with elevated temperature ascends along Fault 1 driven by buoyancy force and ultimately discharges onto the seafloor where it could form a SEDEX-type deposit like the Mount Isa deposit adjacent to the Mount Isa fault. Two convection cells also develop in the aquifer unit near the side boundaries, which is likely due to the impermeable fluid conditions assigned for the sides. Comparison of Figures 2(a) with 2(b) indicates that as time progresses, more cold seawater recharges into the basin and hence cools down the system. As a result, the venting fluid temperature drops from 240℃ at a time of 55 ka to 160℃ at 1 Ma, after which the hydrothermal fluid flow system reaches a steady state (i.e., temperature and fluid velocity no longer vary with time). The venting fluid velocity at steady state is 4.1 m/year.

The second case study considers the same conditions as case 1, except that the faults have been sealed by the uppermost cover sequence to test the concept that stratiform lead-zinc deposits may form by replacement of chemically favorable black shale units below low-permeability cap rocks adjacent to major discharge faults[24]. As shown in Figure 3, no significant marine fluids recharge down into the basin and no venting of hydrothermal fluids at the seafloor. Fluid flow occurs within the aquifer and along the faults to form three 20-km-scale hydrothermal circulation cells: one between the faults and two close to the side boundaries. It is also apparent from Figure 3(b) that significant hydrothermal fluid moves laterally below the uppermost cap-rock layer. Thus, the potential exists for shale-hosted, replacement-style, stratiform Zn deposits to form by this mechanism if a chemically suitable rock type (e.g., organic-rich siltstone or reactive carbonate) is present. However, the fluid flow rates and the fluid temperatures are significantly less than case 1, suggesting that only small and low grade deposits are likely to form by this mechanism.

The third case study involves a scenario that Fault 1 only penetrates 10 km deep (reaching the aquifer only) and Fault 2 remains the same as before (penetrating all the way to the base of the model). All the other conditions are kept the same as those in case 1. As illustrated in Figure 4, numerical results for this model are very similar to those for case 1 (refer to Figure 2(b) and (c)). Again, Fault 1 behaves as the discharge pathway
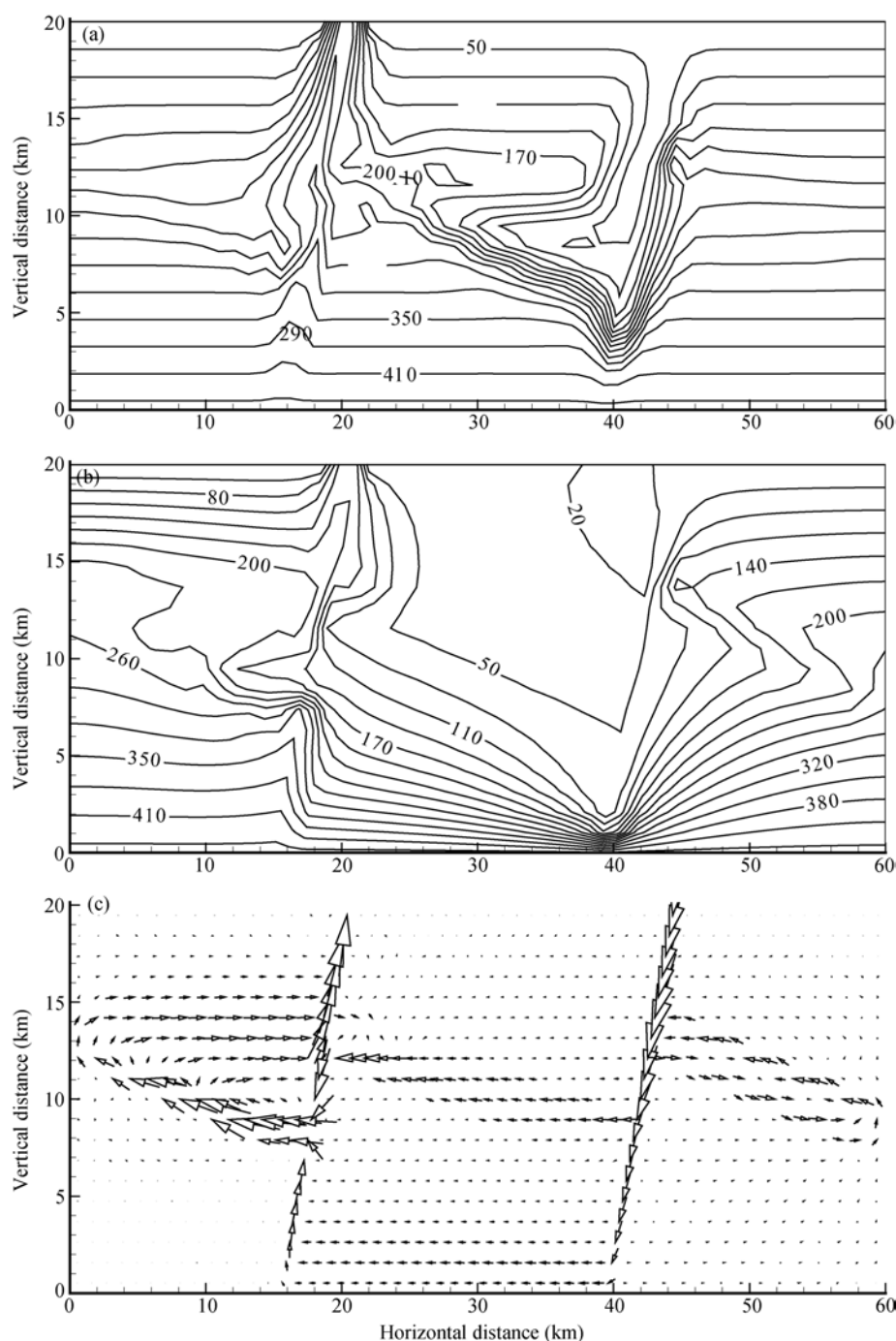
Figure 2 Case 1 corresponding to the reference conditions given in Figure 1 and Table 1. (a) Temperature contours at a time of 55 ka; (b) temperature contours at a time of 1 Ma, after which the hydrothermal system reaches a steady state; (c) fluid velocity vectors at steady state.

and Fault 2 as the recharge pathway. However, the venting fluid temperature at the steady state in this case is 115℃, 45℃ less than that in case 1. This is obviously due to the fact that the discharge fault only penetrates 10 km deep and does not reach the volcanic basement at bottom where temperature is very high. The venting fluid velocity at the steady state is 2.6 m/year.

In the final case study, we assume both the faults to penetrate only 10 km deep, and all the other conditions remain the same as in case 1. Numerical results are shown in Figure 5. It can be seen that unlike the previous scenarios, this hydrological model facilitates and accommodates a 'reversed' recharge-discharge pattern of hydrothermal fluid flow. Fault 1 now acts as the re-
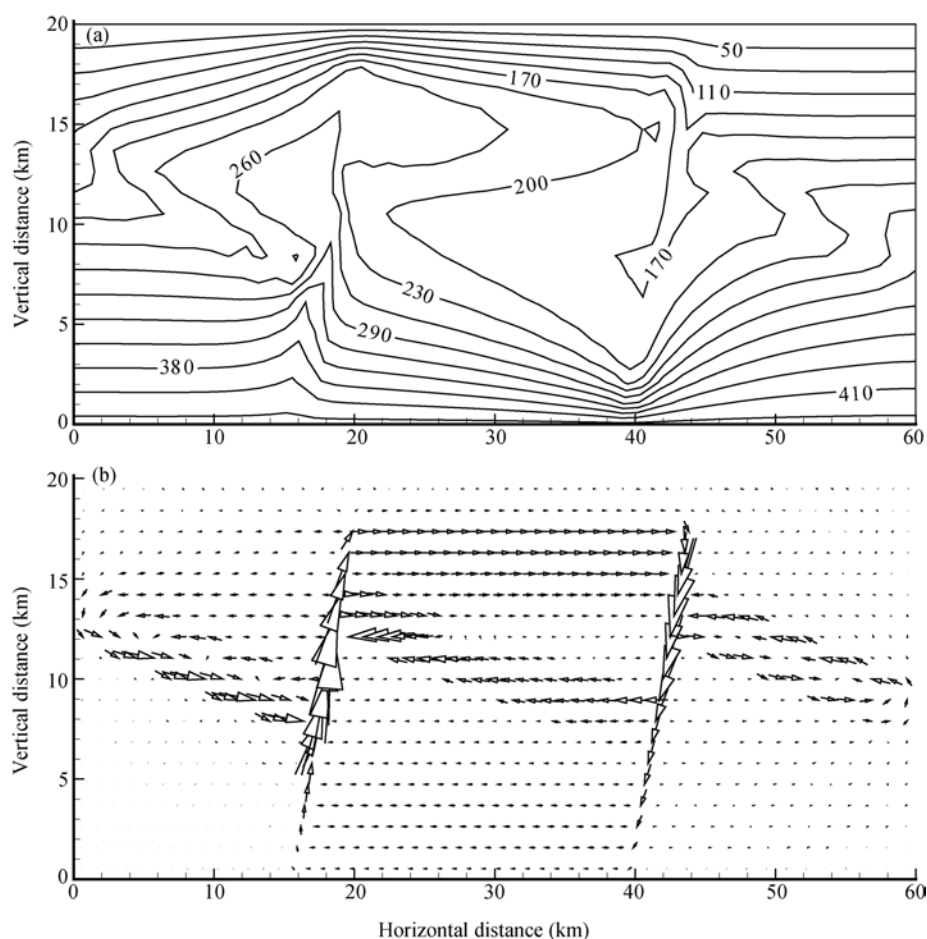
Figure 3 Case 2 corresponding to the condition that the faults have been sealed by the low-permeability uppermost cover sequence. (a) Temperature contours at steady state; (b) fluid velocity vectors at steady state. Note the lack of fluid discharge onto the basin floor.

charge fault and Fault 2 as the discharge fault. Cold seawater moves downwards from the seafloor along Fault 1, and it becomes divergent when reaching the aquifer. Little of the fluid migrates westbound and forms a clock-wise convection cell to the left of the recharge fault; however, most of the fluid travels laterally along the permeable aquifer horizon towards the east side of the model. In the meantime, the thermal energy gained from the lower boundary heats up the fluid and eventually drives it to ascend along Fault 2 and discharge onto the basin floor where it could form a SEDEX-type deposit. The venting fluid temperature and velocity via the discharge fault at the steady state are 142℃ and 3.5 m/year, respectively.

4 Discussion and conclusions

Numerical experiments have been conducted in this study in order to investigate the role of buoyancy force

in the formation of SEDEX-type deposits. The Mount Isa basin in Northern Australia serves as the field setting. Our numerical results corresponding to a highly conceptualized hydrological system have revealed that the interplay between active synsedimentary faults and clastic aquifer units controls the basinal fluid flow and hydrothermal discharge. Marine waters recharge the basin via one fault, move laterally through the clastic aquifer unit where they are heated by the geothermal gradient and leach metals, and then discharge to the surface via the other fault. Convective cells are established, based on the fault spacing and penetration depth. In all of the first three case studies, Fault 1 acted as the discharge conduit and Fault 2 as the recharge conduit. However, when both faults only penetrate down to 10 km deep as discussed in the forth case study, a 'reversed' recharge-discharge pattern of hydrothermal fluid flow developed. The factors causing this change are not fully understood; nevertheless they are more likely controlled
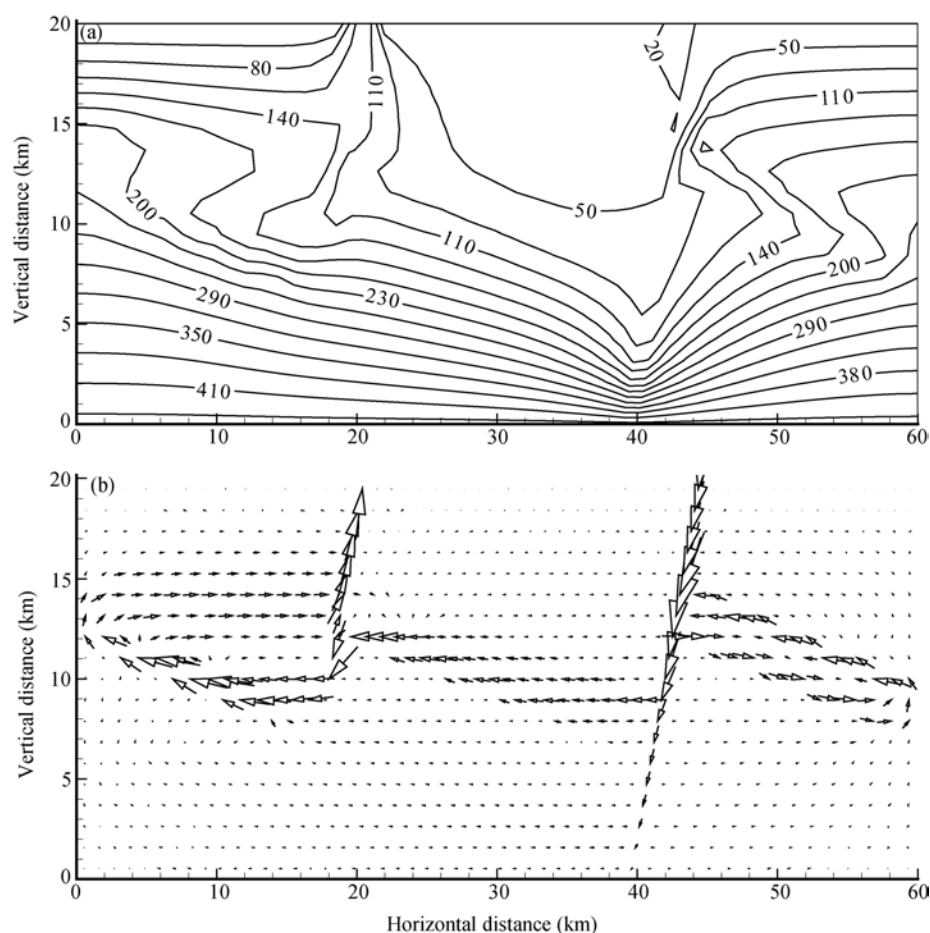
Figure 4 Case 3 corresponding to the condition that Fault 1 only penetrates 10 km deep and Fault 2 remains the same as shown in Figure 1. (a) Temperature contours at steady state; (b) fluid velocity vectors at steady state. Note the venting fluid temperature in this case is lower than that in case 1.

by the basin architecture and its spatial relation with the faults (e.g., Yang et al.[13]). Although noticing the fact that one fault behaves as the recharge conduit and the other as the discharge conduit, or vice versa, we do not intend to investigate the exact reasons leading to a certain recharge-discharge pattern of fluid flow. Rather, this study aims at evaluating the potential of buoyancy force in driving hydrothermal fluid flow associated with the formation of SEDEX-type deposits.

All the numerical case studies described above have confirmed that buoyancy force is indeed an effective and efficient driving mechanism for basin-scale hydrothermal fluid flow. The critical question we need to address is whether the fluid discharge velocities and temperatures predicted by the model have the potential to form world-class supergiant deposits, like the Mount Isa deposit. Our numerical results for different scenarios have revealed that the venting fluid velocities range from 2.6 m/year to 4.1 m/year over a period of 1 Ma. This gives rise to an average discharge fluid flux of about 300 m^3/year per meter of fault strike (noticing the average porosity is 10%). If the Mount Isa deposit formed from fluid discharge from the Mount Isa fault along a fault length of 2000 m, and the discharging fluids were carrying about 100 ppm Zn[25], then the simulated venting fluid has the capacity to form a deposit containing 60 million tonnes of Zn metal over the discharge period of 1 Ma, provided that all the zinc carried in the fluid is precipitated upon exhalation to form the deposit. The defined zinc metal resource of 1.57×10^7 t[1] at the Mount Isa deposit could be accounted for with a metal deposition efficiency of about 26%. Also given the temperature constraint of the Mount Isa mineralization[21-23] and the simulated thermal patterns stated above, cases 1, 3 and 4 seem to be favorable for the formation of a Mount Isa-type ore body adjacent to a major fault system.
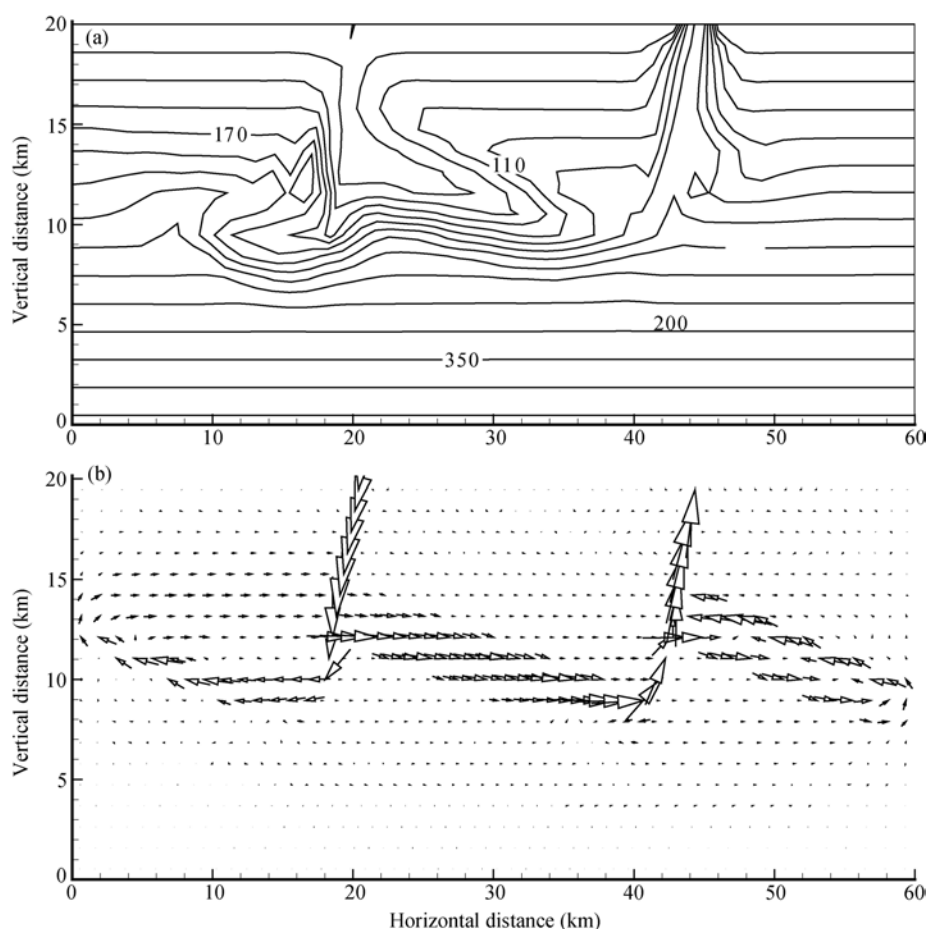
Figure 5 Case 4 corresponding to the condition that both the faults only penetrate 10 km deep. (a) Temperature contours at a time of 55 ka; (b) fluid velocity vectors at steady state. Note Fault 1 now acts as the recharge fault and Fault 2 as the discharge fault.

The numerical modeling studies presented here therefore support the following final conclusion: buoyancy force is an efficient and effective driving mechanism for basin-scale fluid flow and heat transport, and it is viable enough to give rise to the generation of super-giant SEDEX deposits like the Mount Isa deposit, Northern Australia.

1 Goodfellow W D, Lydon J W, Turner R J W. Geology and genesis of stratiform sediment-hosted (Sedex) zinc-lead-silver sulfide deposits. In: Kirkham R V, Sinclair W D, Thorpe R I, et al, eds. Mineral Deposit Modelling. Ottawa: Geological Association of Canada Special Publications, Vol 40, 1993. 201－253

2 Garven G. Continental-scale groundwater flow and geologic processes. Annu Rev Earth Planet Sci, 1995, 24: 89－117

3 Raffensperger J P, Vlassopoulos D. The potential for free and mixed convection in sedimentary basins. Hydrol J, 1999, 7: 505－520

4 Sharp J M, Fenstemaker T R, Simmons C T, et al. Potential salinity-driven free convection in a shale-rich sedimentary basin: Example from the Gulf of Mexico basin in south Texas. Am Assoc Pet Geol Bull, 2001, 85: 2089－2110

5 Fisher A T, Becker K. Correlation between seafloor heat flow and basement relief: Observational and numerical examples and implications for upper crustal permeability. J Geophys Res, 1995, 100: 12641－12657

6 Yang J, Latychev K, Edwards R N. Numerical computation of hydrothermal fluid circulation in fractured earth structures. Geophys J Int, 1998, 135: 627－649

7 Frind E O. Simulation of long-term transient density-dependent transport in groundwater. Adv Water Res, 1982, 5: 73－88

8 Voss C I, Souza W R. Variable density flow and solute transport simulation of regional aquifers containing a narrow freshwater-saltwater transition zone. Water Resour Res, 1987, 23: 1851－1866

9 Therrien R, Sudicky E A. Three-dimensional analysis of variably-saturated flow and solute transport in discretely-fractured porous

media. J Contam Hydrol, 1996, 23: 1−44

10　Shikaze S G, Sudicky E A, Schwartz F W. Density-dependent solute transport in discretely-fractured geological media: Is prediction possible? J Contam Hydrol, 1998, 34: 273−291

11　Solomon M, Heinrich C A. Are high-heat-producing granites essential to the origin of giant lead-zinc deposits at Mount Isa and McArthur River, Australia? Explor Min Geol, 1992, 1: 85−91

12　Garven G, Bull S W, Large R R. Hydrothermal fluid flow models of stratiform ore genesis in the McArthur Basin, Northern Territory, Australia. Geofluids, 2001, 1: 289−312

13　Yang J, Large R R, Bull S W. Factors controlling free thermal convection in faults in sedimentary basins: Implications for the formation of zinc-lead mineral deposits. Geofluids, 2004, 4: 237−247

14　Yang J, Bull S W, Large R R. Numerical investigation of salinity in controlling ore-forming fluid transport in sedimentary basins: Example of the HYC deposit, Northern Australia. Miner Depos, 2004, 39: 622−631

15　Bear J. Dynamics of Fluids in Porous Media. New York: American Elsevier Publishing Company, 1972

16　Huyankorn P S, Pinder G F. Numerical Methods in Subsurface Flow. Toronto: Academic Press, 1983

17　Kinzelbach W K H. Groundwater Modelling —— An Introduction with Sample Programs in BASIC. Amsterdam: Elsevier Science Publisher, 1986

18　Yang J. Finite element modeling of transient saline hydrothermal fluids in multifaulted sedimentary basins: Implications for ore-forming processes. Can J Earth Sci, 2006, 43: 1331−1340

19　O'dea M G, Lister G S, MacCready T, et al. Geodynamic evolution of the Proterozoic Mount Isa terrain. Geol Soc Spec Pub, 1997, 121: 99−122

20　Betts P G, Giles D, Lister G S. Tectonic environment of shale-hosted massive sulfide Pb-Zn-Ag deposits of Proterozoic northeastern Australia. Econ Geol, 2003, 98: 557−576

21　Bierlein F P, Betts P G. The Proterozoic Mount Isa fault zone, northeastern Australia: Is it really a ca. 1.9 Ga terrane-bounding suture? Earth Planet Sci Lett, 2004, 225: 279−294

22　Oliver N H S, McLellan J G, Hobbs B E, et al. Numerical models of extensional deformation, heat transfer, and fluid flow across basement-cover interfaces during basin-related mineralization. Econ Geol, 2006, 101: 1−31

23　McLellan J G, Oliver N H S, Hobbs B E. The relative effects of deformation and thermal advection on fluid pathways in basin-related mineralization. J Geochem Explor, 2006, 89: 271−275

24　Broadbent G C, Myers R E, Wright J V. Geology and origin of shale-hosted Zn Pb-Ag mineralization at the Century deposit, northwest Queensland, Australia. Econ Geol, 1998, 93: 1264−1294

25　Cooke D R, Bull S W, Large R R, et al. The importance of oxidized brines for the formation of Australian Proterozoic stratiform sediment-hosted Pb-Zn (Sedex) deposits. Econ Geol, 2000, 95: 1−18